Prognostic values of GMPS, PR, CD40, and p21 in ovarian cancer

Ping Wang [1] , **Zengli Zhang** [2] , **Yujie Ma** [1] , **Jun Lu** [1] , **Hu Zhao** [1] , **Shuiliang Wang** [1] , **Jianming Tan** [Corresp., 1, 3] , **Bingyan Li** [Corresp. 2]

[1] Fujian Key Laboratory of Transplant Biology, Fuzhou General Hospital, Fuzhou, Fujian, China

[2] Department of Toxicology, School of Public Health, Soochow University, Suzhou, Jiangsu, China

[3] Fujian Hongyi Health Institute, Fuzhou, Fujian, China

Corresponding Authors: Jianming Tan, Bingyan Li
Email address: tanjm156@xmu.edu.cn, bingyanli@suda.edu.cn

Early detection and prediction of prognosis and treatment responses are all the keys in improving survival of ovarian cancer patients. This study profiled an ovarian cancer progression model to identify prognostic biomarkers for ovarian cancer patients. Mouse ovarian surface epithelial cells (MOSECs) can undergo spontaneous malignant transformation *in vitro* cell culture. These were used as a model of ovarian cancer progression for alterations in gene expression and signaling detected using the Illumina HiSeq2000 Next-Generation Sequencing platform and bioinformatical analyses. The differential expression of four selected genes was identified using the gene expression profiling interaction analysis (http://gepia.cancer-pku.cn/) and then associated with survival in ovarian cancer patients using the Cancer Genome Atlas dataset and the online Kaplan-Meier Plotter (www.kmplot.com) data. The data showed 263 aberrantly expressed genes, including 182 up-regulated and 81 down-regulated genes between the early and late stages of tumor progression in MOSECs. The bioinformatic data revealed four genes [i.e., guanosine 5'-monophosphate synthase (GMPS), progesterone receptor (PR), CD40, and p21 (cyclin-dependent kinase inhibitor 1A)] to play an important role in ovarian cancer progression. Furthermore, the Cancer Genome Atlas dataset validated the differential expression of these four genes, which were associated with prognosis in ovarian cancer patients. In conclusion, this study profiled differentially expressed genes using the ovarian cancer progression model and identified four (i.e., GMPS, PR, CD40, and p21) as prognostic markers for ovarian cancer patients. Future studies of prospective patients could further verify the clinical usefulness of this four-gene signature.

1   **Prognostic values of GMPS, PR, CD40, and p21 in ovarian cancer**

3   Ping Wang[1] Zengli Zhang[2] Yujie Ma[1] Jun Lu[1] Hu zhao[1] Shuiliang Wang[1] Jianming Tan[13]

4   Bingyan Li[2]

7   [1]Fujian Key Laboratory of Transplant Biology, Fuzhou General Hospital, Fuzhou, Fujian, China

8   [2]Department of Toxicology, School of Public Health, Soochow University, Jiangsu Suzhou,

9   China

10   [3]Fujian Hongyi Health Institute, Fuzhou, China

12   **Corresponding authors:** Dr. Bingyan Li, Tel.: 86-13771875966; Email: bingyanli@suda.edu.cn

13   Or Dr. Jianming Tan, Tel.: 86-13705005511; Email: tanjm156@xmu.edu.cn

15   **Running title:** Biomarker prediction of ovarian cancer prognosis

Abstract

Early detection and prediction of prognosis and treatment responses are all the keys in improving survival of ovarian cancer patients. This study profiled an ovarian cancer progression model to identify prognostic biomarkers for ovarian cancer patients. Mouse ovarian surface epithelial cells (MOSECs) can undergo spontaneous malignant transformation *in vitro* cell culture. These were used as a model of ovarian cancer progression for alterations in gene expression and signaling detected using the Illumina HiSeq2000 Next-Generation Sequencing platform and bioinformatical analyses. The differential expression of four selected genes was identified using the gene expression profiling interaction analysis (http://gepia.cancer-pku.cn/) and then associated with survival in ovarian cancer patients using the Cancer Genome Atlas dataset and the online Kaplan-Meier Plotter (www.kmplot.com) data. The data showed 263 aberrantly expressed genes, including 182 up-regulated and 81 down-regulated genes between the early and late stages of tumor progression in MOSECs. The bioinformatic data revealed four genes [i.e., guanosine 5'-monophosphate synthase (GMPS), progesterone receptor (PR), CD40, and p21 (cyclin-dependent kinase inhibitor 1A)] to play an important role in ovarian cancer progression. Furthermore, the Cancer Genome Atlas dataset validated the differential expression of these four genes, which were associated with prognosis in ovarian cancer patients. In conclusion, this study profiled differentially expressed genes using the ovarian cancer progression model and identified four (i.e., GMPS, PR, CD40, and p21) as prognostic markers for ovarian cancer patients. Future studies of prospective patients could further verify the clinical usefulness of this four-gene signature.

Introduction

40

41 Ovarian cancer is a lethal disease in women. Epithelial ovarian cancer accounts for

42 approximately 90% of all ovarian malignancies (Siegel et al. 2018) and is frequently diagnosed

43 at the advanced stages when cancer cells have already metastasized to other organs (Jayson et al.

44 2014). For example, ovarian cancer only represents 2.5% of all female malignancies but

45 contributes to 5% of female cancer deaths, indicating a poor 5-year survival rate (Jayson et al.

46 2014). However, if diagnosed early, the 5-year survival rate could reach approximately 93%

47 (Torre et al. 2018). Thus, early tumor detection and effective prognosis prediction are the keys in

48 improving survival of ovarian cancer patients. To this end, previous studies have searched and

49 evaluated biomarkers to diagnose this now deadly disease early and to predict survival or

50 treatment responses or target the biomarker genes to develop novel therapies for ovarian cancer

51 (Jayson et al. 2014) as well as analyzed the differential gene expression patterns between

52 mucinous and clear cell ovarian cancers or between low-grade, low malignant potential and high-

53 grade, metastatic ovarian cancer (Bonome et al. 2005; Meinhold-Heerlein et al. 2005). Other

54 studies associated alterations in gene or gene expression as biomarkers for the early detection or

55 risk assessment of ovarian cancer (Earp et al. 2018; Urban et al. 2018). However, to date, there

56 are no useful or reliable molecular or clinical markers available for such a purpose (Force et al.

57 2018). The current approaches or analyses of differential gene expression profiles usually

58 compare ovarian cancer vs. normal tissues, which leads to limited data; nevertheless, the

59 characterization of differential gene expression profiles between early stage precursor lesions

60 and ovarian cancer could provide novel insights into identifying biomarkers for early detection

61 or prognosis prediction and therapeutic targets of ovarian cancer.

62 We established and characterized an *in vitro* cell model of mouse epithelial ovarian cancer

63 progression according to the method of previous research (Gamwell et al. 2012). This cell model

64 system uses isolated ovarian surface epithelial cells (MOSECs) from mice and cultures them *in*

65 *vitro*. These MOSECs can undergo spontaneous malignant transformation into epithelial ovarian

66 cancer cells (Flesken-Nikitin et al. 2013b; Gamwell et al. 2012; McCloskey et al. 2014; Roberts

67   et al. 2005). During *in vitro* cell culture and passages, the MOSECs show morphology changes

68   and gene alterations (Flesken-Nikitin et al. 2013b; Gamwell et al. 2012; McCloskey et al. 2014;

69   Roberts et al. 2005), which could be a good *in vitro* cell model to mimic human ovary

70   carcinogenesis. Previous studies showed that the spontaneously transformed MOSECs had

71   reliable formation of homologous HGSC tumors. MOSE-I cells refer as a pre-cancerous benign

72   tumor, while MOSE-II cells are malignantly transformed cells (McCloskey et al. 2014).

73   To date, epithelial ovarian cancer has a terrible prognosis and detection of differentially

74   expressed genes (DEGs) in ovarian cancer could better stratify the risk in predicting ovarian

75   cancer in women and/or treatment responses. Thus, in this study, we first isolated MOSECs from

76   six-month female BALB/c mice and continuously cultured and passaged them in more than 35

77   passages, during which we obtained early passaging MOSECs and later passaging MOSECs and

78   named them MOSE-I and MOSE-II, respectively. These MOSE cells model is a credible in

79   research on ovarian cancer because these two types of MOSECs displayed distinguished cell

80   morphology and growth potential in soft agar. We thus utilized them to profile differentially

81   expressed genes using the Illumina HiSeq2000 Next-Generation Sequencing (NGS) platform and

82   bioinformatical analyses and to identify prognostic biomarkers for ovarian cancer patients using

83   the gene expression profiling interaction analysis (GEPIA; http://gepia.cancer-pku.cn/). Our

84   hypothesis was to utilize MOSECs to identify and evaluate DEGs as biomarkers for ovarian

85   cancer early diagnosis and prognosis prediction; thus, we then associated these DEGs with

86   survival of ovarian cancer patients using the Cancer Genome Atlas dataset and the online

87   Kaplan-Meier Plotter (www.kmplot.com) data. We also used the gene ontology (GO) and the

88   Kyoto Encyclopedia of Genes (KEGG) tools to assess the functions of these DEGs for better

89   understanding of ovarian cancer biology.

90

91   **Materials and Methods**

92   *Isolation and culture of MOSE cells*

93   The animal protocol for this study was approved by the Institutional Animal Care and Use

94   Committee (IACUC) of Fuzhou General Hospital (Fujian, China) and followed the regulatory

95 animal care guidelines of the United State National Institute of Health (Bethesda, MD, USA). In

96 this study, we obtained six-month female BALB/c mice from the Shanghai SLAC Laboratory

97 Animal Co., Ltd. (Shanghai, China). We isolated mouse ovarian surface epithelial cells

98 (MOSECs) and cultured them in the "MOSE medium" containing α-Minimum Essential

99 Medium from Thermo-Fisher Scientific Company (Waltham, MA, USA) supplemented with 4%

100 heat-inactivated 3:1 donor bovine serum: fetal bovine serum (Gibco, Gaithersburg, MD, USA), 5

101 U/ml of penicillin and 5 μg/ml of streptomycin solution (Invitrogen, Carlsbad, CA), 0.1 μg/ml

102 of gentamicin (Invitrogen) at 37°C with 5% CO_2 according to the previous described protocols

103 (Gamwell et al. 2012; McCloskey et al. 2014). The MOSECs with spontaneously malignant

104 transformation phenotypes were maintained in the MOSE medium according to a previous study

105 (Flesken-Nikitin et al. 2013a), which have two phases, i.e., the early stage (MOSE-I; normal

106 epithelial cells) and the later stage (MOSE-II; various phenotypes of ovarian cancer cells).

107

108 *Generation and characterization of MOSE-I and MOSE-II cells*

109 To induce spontaneous malignant transformation of MOSECs, we grew and passaged the

110 primary cultured MOSECs in the MOSE medium continuously. The early passages of MOSECs

111 were MOSE-I, whereas MOSECs at 35 passages or more become MOSE-II. To distinguish them,

112 we monitored their morphology under an inverted phase contrast microscope (Thermo-Fisher,

113 Waltham, MA, USA) and grew them in the soft agar. Specifically, cells were passaged from

114 adherent cultures using 0.05% trypsin, washed with phosphate-buffered saline (PBS) to make a

115 single cell suspension by passing cells through a syringe, and then 100 cells were plated into

116 each of the 40-mm cell culture dishes and grown for 14 days. The cells were then stained with

117 crystal violet (Sigma Aldrich Chemicals, St. Louis, MO, USA), photographed under an inverted

118 microscope, and counted. For the soft agar assay, we first made the base layer agar by mixing 1:1

119 of 2×Ham's F-12: the MOSE medium (Sigma Aldrich Chemicals, St. Louis, MO, USA) in 60-

120 mm cell culture dishes and then mixing the cell suspension (2.5×10^4) with the ultrapure LMP

121 agarose (Invitrogen, Carlsbad, CA, USA) at 37°C and then pouring this into the top of the base

122 layer of agar and incubating them at 37°C for 7 days. The cell colonies were photographed using

123 the EVOS XL imaging system (Invitrogen) and quantified using Image J software (National

124 Institute of Heath, Bethesda, MD, USA).

125

126 *Next-generation sequencing of differentially expressed genes between MOSE-I and MOSE-II*

127 *cells*

128 To profile differentially expressed genes between MOSE-I and MOSE-II cells, we performed

129 next-generation sequencing of differentially expressed genes between MOSE-I and MOSE-II

130 cells. In brief, the total cellular RNA was isolated from MOSE-I and MOSE-II cells using Trizol

131 Reagent (Invitrogen) according to the manufacturer's protocol. After RNA quantitation and

132 reverse transcription into cDNA, we prepared the cDNA library for each cell type using Illumina

133 TruSeq Libraries (Illumina, #RS-122-2001, NY USA) and then performed next-generation

134 sequencing of differentially expressed genes between MOSE-I and MOSE-II cells using the

135 Illumina HiSeq2000 NGS platform available at Tigem Institute in Pozzuoli (Naples).

136

137 *Bioinformatic analysis with the Gene Ontology (GO) terms and the Kyoto Encyclopedia of*

138 *Genes and Genomes (KEGG) database*

139 These differentially expressed genes (DEGs) were bioinformatically analyzed using the GO term

140 to annotate the unique biological functions of these DEGs. We then further analyzed their

141 signaling in the pathways using the KEGG database. The significant GO terms and pathways

142 were generated using Fisher's exact test and statistically corrected using the false discovery rate

143 (FDR) of the *p*-values.

144

145 *Construction of DEGs into a protein-protein interaction (PPI) network*

146 After bioinformatic analysis of these DEGs with the GO terms and the KEGG database, we

147 further constructed these DEGs into the PPI network using STRING (version 9.1,

148 http://www.string-db.org/) according to the previous description (Franceschini et al. 2013). This

149 web resource contains a biological database for the comprehensive prediction of the known

150 protein-protein interactions. We uploaded our DEGs into the STRING database; the web site

151 then generated the PPIs for these DEGs. We used a combined score of > 0.5 as the cut-off

152 criterion to identify any given protein interacts with another one and then imported these PPI

153 pairs into the Cytoscape software (http://www.cytoscape.org/) according to previous research

154   (Saito et al. 2012) to help us to construct the PPI network, in which the hub nodes (the key

155   proteins that possess important biological functions) were revealed by calculating the degree to

156   connect to other proteins vs. non-connected ones.

157

158   *Gene expression profiling interaction analysis (GEPIA)*

159   GEPIA is a web tool (http://gepia.cancer-pku.cn/) to profile gene expressions between tumor and

160   non-tumor tissues and provides interactive data analyses. In this study, we utilized this online

161   tool to analyze the levels of four selected DEGs (i.e., GMPS, PR, CD40, and p21) between

162   ovarian cancer specimens and normal controls and performed a Student's t-test to for statistical

163   significance with a cut-off of p value <0.05 and four-fold changes.

164

165   *The TCGA database and cBioPortal*

166   The Cancer Genome Atlas database was used to store both DEGs and clinicopathological data on

167   30 different human cancers (Tomczak et al. 2015). In this study, we retrieved the ovary invasive

168   carcinoma (TCGA, Provisional) dataset, which includes DEGs data on 606 cases of ovarian

169   cancer vs. 311 normal tissues. We then put our DEGs data vs. TCGA data into the cBioPortal

170   (www.cbioportal.org), which is a web resource to help explore, visualize, and analyze DEGs data

171   (Gao et al. 2013). The overall survival (OS) and disease-free survival (DFS) were stratified by

172   these DEGs and then calculated according to the cBioPortal's online instructions. In addition, we

173   also generated the Kaplan-Meier curves of ovarian cancer patients stratified by the expression of

174   GMPS, PR, Cd40, and p21 mRNA levels using the online Kaplan-Meier Plotter

175   (www.kmplot.com) according to a previous study (Gyorffy et al. 2013). This website

176   accumulated data on the gene expression and survival of 4,142 ovary cancer patients. We

177   analyzed the relapse-free survival (RFS) of ovarian cancer patients stratified by high vs. low

178   expression of GMPS, PR, CD40, and p21 using the Kaplan-Meier curves and the log rank test

179   and the hazard ratio with 95% confidence intervals (CI). The reason to select these four top hub

180   genes was because they possessed a number-at-risk below the main plot (curve).

181

182 **Results**

183 *Characterization of MOSE-I and MOSE-II cells*

184 In this study, we isolated MOSECs from female BALB/c mice and passaged them into MOSE-I

185 and MOSE-II cells *in vitro*. We found that the early passages of MOSE-I cells grew slowly with

186 doubling time of 48 h, whereas the growth rate MOSE-I increased when it was passaged more

187 than 35 passages. Morphologically, MOSE-I cells started to lose the epithelial "cobblestone"-like

188 appearance under an inverted microscope, which is the characteristic of early passage MOSE-I

189 cells (Figure 1A), consistent with previous studies (Gamwell et al. 2012; McCloskey et al. 2014).

190 Continual passaging of MOSE-I for more than 35 passages led it to be established as MOSE-II.

191 MOSE-II loses the epithelial "cobblestone"-like morphology and transitions to a more

192 mesenchymal morphology (Figure 1A). To distinguish them, we monitored their morphology

193 under an inverted phase contrast microscope and grew them in soft agar. The latter assay

194 measures the anchorage-independent growth, which is the characteristic of transformed cells *in*

195 *vitro*. Our data showed that MOSE-II cells were able to form colonies in the soft agar, whereas

196 MOSE-I could not (Figure 1BD). We also assessed their proliferation capacity using the plate

197 colony formation assay and found that MOSE-II formed more colonies with larger cell sizes than

198 those of MOSE-I cells (Figure 1CEF).

199

200 *Profiling of differentially expressed genes (DEGs) between MOSE-I and MOSE-II cells*

201 Using this cell model of MOSE-I and II, we profiled DEGs using the Illumina HiSeq2000 NGS

202 platform. Our experiments were in three biological replicates to reduce sample variations due to

203 cell heterogeneous cultures. MOSE-I cells were randomly selected at Passage 5 (P5), P15, and

204 P25, respectively, while MOSE-II cells were selected at P50, P70 and P90, respectively. Among

205 them, 14218 genes were detected and analyzed. We found a total of 263 DEGs, which included

206 182 up-regulated and 81 down-regulated DEGs using Volcano plots (Figure 2). The cut-off

207   values for the up-regulated DEGs were log2 FC > 2 and p < 0.05, while the down-regulated

208   DEGs were log2FC<-2, p <0.05 (Table 1).

209

210   *Bioinformatical data on the GO terms, KEGG, and PPI network of the DEGs*

211   The GO terms showed that these DEGs formed several important terms in cell biology, such as

212   positive regulation of cell proliferation, positive regulation of transcription from RNA

213   polymerase II promoter and signal transduction (Figure 3B). The KEGG pathway analysis

214   showed that these DEGs-formed hub genes were enriched in the pathways related to the PI3K-

215   Akt signaling and pathways in cancer (Figure 3A), both of which are positively associated with

216   ovarian cancer development (Kurose et al. 2001; Li et al. 2014; Rossig et al. 2001). Furthermore,

217   the PPI network of these DEGs is shown in Figure 4. In particular, there were 35 nodes forming

218   the hub genes from 27 up-regulated and 8 down-regulated genes (Table 2).

219

220   *Association of these DEGs-formed hub gene expressions with overall survival of ovarian cancer*

221   *patients*

222   We then associated the expression of these DEGs-formed hub genes with OS and DFS of ovarian

223   cancer patients using TCGA database data. We first assessed the expression of all 35 hub genes

224   in 182 tissue samples out of 263 ovary invasive cancer patients and found that among these

225   genes, four (GMPS, PR, CD40, and p21) had the alteration rates of more than 10% (Figure 5A).

226   We then plotted the Kaplan-Meier curves and performed a log-rank test to associate them with

227   OS and DFS of patients. Our data showed that the aberrant expression of GMPS, PR, CD40, and

228   p21 mRNA was associated with poorer OS in patients (Figure 5B) but not with DFS in patients

229   (Figure 5C).

230   Indeed, these four genes were also differentially expressed in ovarian cancer tissues vs.

231   normal tissues; specifically, GMPS was highly expressed in ovary cancer tissues (Figure 6A),

232   which was associated with RFS in patients (Figure 6E). In contrast, the expression of PR, CD40,

233   and p21 mRNA was reduced in ovarian cancer tissues (Figure 6BCD), which was associated

234 with poor RFS (Figure 6FGH).

235

236 **Discussion**

237 In the current study, we profiled DEGs between pre-malignant MOSE-I and highly malignant

238 MOSE-II cells and found 182 up-regulated and 81 down-regulated DEGs. Our bioinformatical

239 analysis showed that these DEGs function to positively regulate cell proliferation, gene

240 transcription from RNA polymerase II promoter, and signal transduction, while KEGG pathway

241 data showed that these DEGs could be related to the PI3K-Akt signaling and pathways in cancer.

242 Furthermore, the PPI network analysis of these DEGs identified 35 hub genes (27 up-regulated

243 and 8 down-regulated genes) and that four of them were associated with poor overall survival in

244 ovarian cancer patients. In addition, these four genes were also differentially expressed in

245 ovarian cancer tissues compared with human normal tissues. Specifically, GMPS was highly

246 expressed in ovary cancer tissues, which was associated with RFS, whereas the expression of PR,

247 CD40, and p21 mRNA was reduced in ovarian cancer tissues, which was associated with poor

248 RFS. In conclusion, the data from the current study profiled and identified four DEGs, which

249 could predict overall survival and recurrence-free survival in ovarian cancer patients. Future

250 prospective study will need to validate our current data before using them clinically. Indeed, this

251 *in vitro* cell model of ovarian cancer progression could provide a useful tool for identifying gene

252 alterations and drug effect tests. In this system, MOSEs cultured *in vitro* can undergo

253 spontaneously malignant transformation into ovarian cancer (McCloskey et al. 2014).

254 Morphologically, MOSE-II cells lost their normal epithelia "cobblestone" characteristic and

255 were able to form soft agar colonies (McCloskey et al. 2014) as well as gene alterations (Lv et al.

256 2012; Roby et al. 2000; Urzua et al. 2010). When MOSE-II cells were injected into the

257 peritoneal cavity of immunodeficient animals, tumor metastases and bloody ascites formed in the

258 mouse peritoneal cavity (Roberts & Schmelz 2013; Roby et al. 2000), which is typical of

259 advanced human ovarian cancer (Ahmed & Stenvers 2013). In 2014, McCloskey and his

260 colleagues discovered that differentially expressed genes of MOSE-II were consistent with the

261 differential genes of human high-grade serous ovarian cancer (HGSC) tumor samples and

262 previous studies of ovarian cancer cell lines (McCloskey et al. 2014). HGSC tumors after

263 immunohistochemical profiles confirmed that MOSE-II can be used as a homologous model of

264 HGSC. Finally, MOSE-II expressing SCA1 appeared to be more aggressive than ovarian cancer

265 cell lines, with increased colony formation efficiency *in vitro* and faster onset of tumors *in vivo*

266 (McCloskey et al. 2014). Thus, this model of cells is useful in the future study of ovarian cancer

267 prevention and treatment (Ricci et al. 2013). In the current study, we profiled DEGs between

268 MOSE-I and MOSE-II cells using this model system and found that DEGs were compatible with

269 human disease. Furthermore, our PPI network analysis identified that 35 significant nodes and

270 nine genes participate in the PI3K-Akt signaling pathway, which confirmed data from a previous

271 study, indicating potential therapeutic targets for ovarian cancer (Li et al. 2014). These genes are

272 frequently altered, such as PIK3CA mutation or amplification in up to 30% ovarian cancer

273 patients, while PTEN expression was lost in up to 40% of patients (Campbell et al. 2004; Kurose

274 et al. 2001). In addition, six of these 35 hub genes are a part of the Rap1 signal pathway, and a

275 previous study reported them to be associated with serous ovarian cancer metastasis (Che et al.

276 2015).

277   Furthermore, these DEGs were annotated into the GO terms and were shown to positively

278 regulate cell proliferation, which is one of six essential cancer hallmarks: self-sufficiency in

279 growth signals (Hanahan & Weinberg 2000). Indeed, the positive regulation of cell proliferation

280 is the basis of cancer development and progression. Moreover, each of these pathways identified

281 in the current study can promote or transform normal cells into cancer cells (Evan & Vousden

282 2001). Furthermore, our current study identified a four-gene signature to predict overall survival

283 of ovarian cancer patients. Specifically, GMPS, a guanosine 5'-monophosphate synthase, is an

284 enzyme that converts xanthosine monophosphate to guanosine monophosphate. Thus, GMPS is

285 important in nucleotide biosynthesis for normal cell proliferation and oncogenesis. Reddy's data

286 showed that GMPS in combination of TRIM21 with USP7 formed a molecular cascade that

287 controls p53 stability in response to DNA damage or nucleotide deprivation. Therefore, GMPS is

288   a classical biosynthetic enzyme that promotes cell growth and DNA replication, and is also a key

289   center for p53-restricted cell proliferation (Reddy et al. 2014). In our current study, we found that

290   GMPS was highly expressed in ovary cancer tissues compared with that of non-tumor tissues and

291   that GMPS expression was associated with RFS of patients. This piece of data is novel and has

292   been not reported in literature before. A previous study showed that GMPS was an important p53

293   repression target in liver cancer cells (Holzer et al. 2017), which further indicates the importance

294   of GMPS in oncogenesis. As we know, p53 is a tumor suppressor protein and can prevent

295   aberrant cell proliferation, which may be through the repression of GMPS activity (Holzer et al.

296   2017). In addition, PR, as the nuclear receptor, functions to regulate the development and cycle

297   of hormone-responsive tissues, such as the mammary glands and reproductive tract. Several

298   previous studies demonstrated PR expression as a biomarker to predict better prognosis of

299   endometrioid and high-grade serous ovarian carcinoma (Jonsson et al. 2015; Lee et al. 2005;

300   Lenhard et al. 2012; Sieh et al. 2013), while lost PR expression was associated with advanced

301   stages of ovarian cancer (Feng et al. 2016). Indeed, progesterone and progestin were shown to

302   play a protective role against ovarian carcinogenesis (Edmondson & Monaghan 2001), and PR

303   expression was a favorable prognostic marker associated with longer progression-free survival in

304   ovarian cancer patients (Tangjitgamol et al. 2009; van Kruchten et al. 2015; Wong et al. 2007).

305   Our current data confirm these previous data. Furthermore, CD40 is a transmembrane

306   glycoprotein and the member of the tumor necrosis factor receptor superfamily, which can

307   mediate a broad variety of immune and inflammatory responses (Grewal & Flavell 1998). CD40

308   is frequently expressed in different immune cells and endothelial and epithelial cells. The

309   binding of CD40 to CD40 ligand was shown to have various physiological and pathological roles

310   in the human body (Grewal & Flavell 1998; van Kooten & Banchereau 2000). A previous study

311   demonstrated that CD40 ligands enhanced the sensitivity of epithelial ovarian cancer cells to

312   cisplatin treatment (Qin et al. 2016). CD40 was highly expressed in ovarian cancer cell lines and

313   tumor samples but not in normal ovarian tissue (Zhou et al. 2012). In our current study, we found

314   elevated CD40 expression in MOSE-II cells compared with MOSE-I cells; however, CD40

315   expression was reduced in ovarian cancer tissues, which is opposite the findings of a previous

316   study (Zhou et al. 2012). Thus, further study is needed to determine the reason for this

317   discrepancy. In addition, p21 also called as CDKN1A cyclin-dependent kinase inhibitor 1A,

318   functions to regulate cell growth arrest by inhibiting Cdks, which is required for cell cycle

319   transition from the G1 to S phase (Xiong et al. 1993). Through the interaction with the

320   proliferating cell nuclear antigen (PCNA),/p21 was able to inhibit DNA replication (Rossig et al.

321   2001). Our current study showed that p21 was highly expressed in normal tissues but reduced in

322   ovarian cancer tissues, which was associated with better survival of patients, consistent with a

323   previous study (Alves et al. 2018). Indeed, a previous study demonstrated that pyridine

324   derivative-induced ovarian cancer cell senescence occurred through p21 activation (Shang et al.

325   2018). However, other studies reported that CDKN1A/p21 expression promoted breast cancer

326   and mediated drug resistance (Cheng et al. 2010; Hawthorne et al. 2009), and clinical studies

327   have indicated that high p21 expression was correlated with poor prognosis of gastric and

328   esophageal cancers (Liu et al. 2014; Taghavi et al. 2010). Thus, further study is needed to clarify

329   this discrepancy.

330   However, our current study does have some limitations; for example, our current study just

331   profiled differentially expressed genes in ovarian cancer and associated them with prognosis of

332   ovarian cancer as well as performed bioinformatical analysis to associate four of them with

333   ovarian cancer progression; however, much more are needed in precise research on their

334   biological functions and role in ovarian cancer development and progression. Furthermore,

335   future validation of these DEGs in ovarian cancer is also needed before any applications to

336   patients.

337

338   **Conclusions**

339   Our current study revealed a four-gene signature after profiling a cell model of ovarian cancer

340   progression to predict overall survival and recurrence-free survival in ovarian cancer patients.

341   Future study will verify these data using prospective ovarian cancer patients.

342

References

343

344

345 **Ahmed N, and Stenvers KL. 2013.** Getting to know ovarian cancer ascites: opportunities for targeted therapy-
346   based translational research. *Front Oncol* **3(**256 DOI:10.3389/fonc.2013.00256.
347 **Alves MR, NC EM, Barros-Filho MC, do Amaral NS, Silva FIB, Baiocchi Neto G, Soares FA, de Brot
348   Andrade L, and Rocha RM. 2018.** Downregulation of AGR2, p21, and cyclin D and alterations in p53
349   function were associated with tumor progression and chemotherapy resistance in epithelial ovarian carcinoma.
350   *Cancer Med* DOI:10.1002/cam4.1530.
351 **Bonome T, Lee JY, Park DC, Radonovich M, Pise-Masison C, Brady J, Gardner GJ, Hao K, Wong WH,
352   Barrett JC, Lu KH, Sood AK, Gershenson DM, Mok SC, and Birrer MJ. 2005.** Expression profiling of
353   serous low malignant potential, low-grade, and high-grade tumors of the ovary. *Cancer Res* **65(22)**:10602-
354   10612 DOI:10.1158/0008-5472.CAN-05-2240.
355 **Campbell IG, Russell SE, Choong DY, Montgomery KG, Ciavarella ML, Hooi CS, Cristiano BE, Pearson RB,
356   and Phillips WA. 2004.** Mutation of the PIK3CA gene in ovarian and breast cancer. *Cancer Res* **64(21)**:7678-
357   7681 DOI:10.1158/0008-5472.CAN-04-2933.
358 **Che YL, Luo SJ, Li G, Cheng M, Gao YM, Li XM, Dai JM, He H, Wang J, Peng HJ, Zhang Y, Li WY, Wang
359   H, Liu B, and Linghu H. 2015.** The C3G/Rap1 pathway promotes secretion of MMP-2 and MMP-9 and is
360   involved in serous ovarian cancer metastasis. *Cancer Lett* **359(2)**:241-249 DOI:10.1016/j.canlet.2015.01.019.
361 **Cheng X, Xia W, Yang JY, Hsu JL, Chou CK, Sun HL, Wyszomierski SL, Mills GB, Muller WJ, Yu D, and
362   Hung MC. 2010.** Activation of p21(CIP1/WAF1) in mammary epithelium accelerates mammary tumorigenesis
363   and promotes lung metastasis. *Biochem Biophys Res Commun* **403(1)**:103-107 DOI:10.1016/j.bbrc.2010.10.126.
364 **Earp M, Tyrer JP, Winham SJ, Lin HY, Chornokur G, Dennis J, Aben KKH, Anton-Culver H, Antonenkova
365   N, Bandera EV, Bean YT, Beckmann MW, Bjorge L, Bogdanova N, Brinton LA, Brooks-Wilson A,
366   Bruinsma F, Bunker CH, Butzow R, Campbell IG, Carty K, Chang-Claude J, Cook LS, Cramer DW,
367   Cunningham JM, Cybulski C, Dansonka-Mieszkowska A, Despierre E, Doherty JA, Dork T, du Bois A,
368   Durst M, Easton DF, Eccles DM, Edwards RP, Ekici AB, Fasching PA, Fridley BL, Gentry-Maharaj A,
369   Giles GG, Glasspool R, Goodman MT, Gronwald J, Harter P, Hein A, Heitz F, Hildebrandt MAT,
370   Hillemanns P, Hogdall CK, Hogdall E, Hosono S, Iversen ES, Jakubowska A, Jensen A, Ji BT, Jung AY,
371   Karlan BY, Kellar M, Kiemeney LA, Kiong Lim B, Kjaer SK, Krakstad C, Kupryjanczyk J, Lambrechts
372   D, Lambrechts S, Le ND, Lele S, Lester J, Levine DA, Li Z, Liang D, Lissowska J, Lu K, Lubinski J,
373   Lundvall L, Massuger L, Matsuo K, McGuire V, McLaughlin JR, McNeish I, Menon U, Milne RL,
374   Modugno F, Moysich KB, Ness RB, Nevanlinna H, Odunsi K, Olson SH, Orlow I, Orsulic S, Paul J,
375   Pejovic T, Pelttari LM, Permuth JB, Pike MC, Poole EM, Rosen B, Rossing MA, Rothstein JH,
376   Runnebaum IB, Rzepecka IK, Schernhammer E, Schwaab I, Shu XO, Shvetsov YB, Siddiqui N, Sieh W,
377   Song H, Southey MC, Spiewankiewicz B, Sucheston-Campbell L, Tangen IL, Teo SH, Terry KL,
378   Thompson PJ, Thomsen L, Tworoger SS, van Altena AM, Vergote I, Vestrheim Thomsen LC, Vierkant
379   RA, Walsh CS, Wang-Gohrke S, Wentzensen N, Whittemore AS, Wicklund KG, Wilkens LR, Woo YL,
380   Wu AH, Wu X, Xiang YB, Yang H, Zheng W, Ziogas A, Lee AW, Pearce CL, Berchuck A, Schildkraut
381   JM, Ramus SJ, Monteiro ANA, Narod SA, Sellers TA, Gayther SA, Kelemen LE, Chenevix-Trench G,
382   Risch HA, Pharoah PDP, Goode EL, and Phelan CM. 2018.** Variants in genes encoding small GTPases and

383   association with epithelial ovarian cancer susceptibility. *PLoS One* **13(7)**:e0197561
384   DOI:10.1371/journal.pone.0197561.

385 **Edmondson RJ, and Monaghan JM. 2001.** The epidemiology of ovarian cancer. *Int J Gynecol Cancer* **11(6)**:423-
386   429

387 **Evan GI, and Vousden KH. 2001.** Proliferation, cell cycle and apoptosis in cancer. *Nature* **411(6835)**:342-348
388   DOI:10.1038/35077213.

389 **Feng Z, Wen H, Bi R, Ju X, Chen X, Yang W, and Wu X. 2016.** A clinically applicable molecular classification
390   for high-grade serous ovarian cancer based on hormone receptor expression. *Sci Rep* **6(**25408
391   DOI:10.1038/srep25408.

392 **Flesken-Nikitin A, Hwang C-I, Cheng C-Y, Michurina TV, Enikolopov G, and Nikitin AY. 2013a.** Ovarian
393   surface epithelium at the junction area contains a cancer-prone stem cell niche. *Nature* **495(7440)**:241-245

394 **Flesken-Nikitin A, Hwang CI, Cheng CY, Michurina TV, Enikolopov G, and Nikitin AY. 2013b.** Ovarian
395   surface epithelium at the junction area contains a cancer-prone stem cell niche. *Nature* **495(7440)**:241-245
396   DOI:10.1038/nature11979.

397 **Force USPST, Grossman DC, Curry SJ, Owens DK, Barry MJ, Davidson KW, Doubeni CA, Epling JW, Jr.,**
398   **Kemper AR, Krist AH, Kurth AE, Landefeld CS, Mangione CM, Phipps MG, Silverstein M, Simon MA,**
399   **and Tseng CW. 2018.** Screening for Ovarian Cancer: US Preventive Services Task Force Recommendation
400   Statement. *Jama* **319(6)**:588-594 DOI:10.1001/jama.2017.21926.

401 **Franceschini A, Szklarczyk D, Frankild S, Kuhn M, Simonovic M, Roth A, Lin J, Minguez P, Bork P, von**
402   **Mering C, and Jensen LJ. 2013.** STRING v9.1: protein-protein interaction networks, with increased coverage
403   and integration. *Nucleic Acids Res* **41(Database issue)**:D808-815 DOI:10.1093/nar/gks1094.

404 **Gamwell LF, Collins O, and Vanderhyden BC. 2012.** The mouse ovarian surface epithelium contains a
405   population of LY6A (SCA-1) expressing progenitor cells that are regulated by ovulation-associated factors. *Biol*
406   *Reprod* **87(4)**:80 DOI:10.1095/biolreprod.112.100347.

407 **Gao J, Aksoy BA, Dogrusoz U, Dresdner G, Gross B, Sumer SO, Sun Y, Jacobsen A, Sinha R, Larsson E,**
408   **Cerami E, Sander C, and Schultz N. 2013.** Integrative analysis of complex cancer genomics and clinical
409   profiles using the cBioPortal. *Sci Signal* **6(269)**:pl1 DOI:10.1126/scisignal.2004088.

410 **Grewal IS, and Flavell RA. 1998.** CD40 and CD154 in cell-mediated immunity. *Annu Rev Immunol* **16(**111-135
411   DOI:10.1146/annurev.immunol.16.1.111.

412 **Gyorffy B, Surowiak P, Budczies J, and Lanczky A. 2013.** Online survival analysis software to assess the
413   prognostic value of biomarkers using transcriptomic data in non-small-cell lung cancer. *PLoS One* **8(12)**:e82241
414   DOI:10.1371/journal.pone.0082241.

415 **Hanahan D, and Weinberg RA. 2000.** The hallmarks of cancer. *Cell* **100(1)**:57-70

416 **Hawthorne VS, Huang WC, Neal CL, Tseng LM, Hung MC, and Yu D. 2009.** ErbB2-mediated Src and signal
417   transducer and activator of transcription 3 activation leads to transcriptional up-regulation of p21Cip1 and
418   chemoresistance in breast cancer cells. *Mol Cancer Res* **7(4)**:592-600 DOI:10.1158/1541-7786.MCR-08-0316.

419 **Holzer K, Drucker E, Roessler S, Dauch D, Heinzmann F, Waldburger N, Eiteneuer EM, Herpel E,**
420   **Breuhahn K, Zender L, Schirmacher P, Ori A, and Singer S. 2017.** Proteomic Analysis Reveals GMP
421   Synthetase as p53 Repression Target in Liver Cancer. *Am J Pathol* **187(2)**:228-235
422   DOI:10.1016/j.ajpath.2016.09.022.

423 **Jayson GC, Kohn EC, Kitchener HC, and Ledermann JA. 2014.** Ovarian cancer. *Lancet* **384(9951)**:1376-1388

424   DOI:10.1016/S0140-6736(13)62146-7.

425   **Jonsson JM, Skovbjerg Arildsen N, Malander S, Masback A, Hartman L, Nilbert M, and Hedenfalk I. 2015.**
426   Sex Steroid Hormone Receptor Expression Affects Ovarian Cancer Survival. *Transl Oncol* **8(5)**:424-433
427   DOI:10.1016/j.tranon.2015.09.002.

428   **Kurose K, Zhou XP, Araki T, Cannistra SA, Maher ER, and Eng C. 2001.** Frequent loss of PTEN expression is
429   linked to elevated phosphorylated Akt levels, but not associated with p27 and cyclin D1 expression, in primary
430   epithelial ovarian carcinomas. *Am J Pathol* **158(6)**:2097-2106 DOI:10.1016/S0002-9440(10)64681-0.

431   **Lee P, Rosen DG, Zhu C, Silva EG, and Liu J. 2005.** Expression of progesterone receptor is a favorable
432   prognostic marker in ovarian cancer. *Gynecol Oncol* **96(3)**:671-677 DOI:10.1016/j.ygyno.2004.11.010.

433   **Lenhard M, Tereza L, Heublein S, Ditsch N, Himsl I, Mayr D, Friese K, and Jeschke U. 2012.** Steroid hormone
434   receptor expression in ovarian cancer: progesterone receptor B as prognostic marker for patient survival. *BMC*
435   *cancer* **12(**553 DOI:10.1186/1471-2407-12-553.

436   **Li H, Zeng J, and Shen K. 2014.** PI3K/AKT/mTOR signaling pathway as a therapeutic target for ovarian cancer.
437   *Arch Gynecol Obstet* **290(6)**:1067-1078 DOI:10.1007/s00404-014-3377-3.

438   **Liu X, Yu H, Cai H, and Wang Y. 2014.** Expression of CD24, p21, p53, and c-myc in alpha-fetoprotein-producing
439   gastric cancer: Correlation with clinicopathologic characteristics and survival. *J Surg Oncol* **109(8)**:859-864
440   DOI:10.1002/jso.23599.

441   **Lv L, Zhang T, Yi Q, Huang Y, Wang Z, Hou H, Zhang H, Zheng W, Hao Q, Guo Z, Cooke HJ, and Shi Q.**
442   **2012.** Tetraploid cells from cytokinesis failure induce aneuploidy and spontaneous transformation of mouse
443   ovarian surface epithelial cells. *Cell Cycle* **11(15)**:2864-2875 DOI:10.4161/cc.21196.

444   **McCloskey CW, Goldberg RL, Carter LE, Gamwell LF, Al-Hujaily EM, Collins O, Macdonald EA, Garson**
445   **K, Daneshmand M, Carmona E, and Vanderhyden BC. 2014.** A new spontaneously transformed syngeneic
446   model of high-grade serous ovarian cancer with a tumor-initiating cell population. *Front Oncol* **4(**53
447   DOI:10.3389/fonc.2014.00053.

448   **Meinhold-Heerlein I, Bauerschlag D, Hilpert F, Dimitrov P, Sapinoso LM, Orlowska-Volk M, Bauknecht T,**
449   **Park TW, Jonat W, Jacobsen A, Sehouli J, Luttges J, Krajewski M, Krajewski S, Reed JC, Arnold N,**
450   **and Hampton GM. 2005.** Molecular and prognostic distinction between serous ovarian carcinomas of varying
451   grade and malignant potential. *Oncogene* **24(6)**:1053-1065 DOI:10.1038/sj.onc.1208298.

452   **Qin L, Qiu H, Zhang M, Zhang F, Yang H, Yang L, Jia L, Qin K, Jia L, Dou X, Cheng L, Sang M, Zhang C,**
453   **Shan B, and Zhang Z. 2016.** Soluble CD40 ligands sensitize the epithelial ovarian cancer cells to cisplatin
454   treatment. *Biomed Pharmacother* **79(**166-175 DOI:10.1016/j.biopha.2016.01.006.

455   **Reddy BA, van der Knaap JA, Bot AG, Mohd-Sarip A, Dekkers DH, Timmermans MA, Martens JW,**
456   **Demmers JA, and Verrijzer CP. 2014.** Nucleotide biosynthetic enzyme GMP synthase is a TRIM21-
457   controlled relay of p53 stabilization. *Mol Cell* **53(3)**:458-470 DOI:10.1016/j.molcel.2013.12.017.

458   **Ricci F, Broggini M, and Damia G. 2013.** Revisiting ovarian cancer preclinical models: implications for a better
459   management of the disease. *Cancer Treat Rev* **39(6)**:561-568 DOI:10.1016/j.ctrv.2013.01.005.

460   **Roberts PC, Mottillo EP, Baxa AC, Heng HH, Doyon-Reale N, Gregoire L, Lancaster WD, Rabah R, and**
461   **Schmelz EM. 2005.** Sequential molecular and cellular events during neoplastic progression: a mouse syngeneic
462   ovarian cancer model. *Neoplasia* **7(10)**:944-956

463   **Roberts PC, and Schmelz EM. 2013.** In vitro model of spontaneous mouse OSE transformation. *Methods Mol Biol*
464   **1049(**393-408 DOI:10.1007/978-1-62703-547-7_30.

465   Roby KF, Taylor CC, Sweetwood JP, Cheng Y, Pace JL, Tawfik O, Persons DL, Smith PG, and Terranova
466   PF. 2000. Development of a syngeneic mouse model for events related to ovarian cancer. *Carcinogenesis*
467   **21(4)**:585-591

468   Rossig L, Jadidi AS, Urbich C, Badorff C, Zeiher AM, and Dimmeler S. 2001. Akt-dependent phosphorylation
469   of p21(Cip1) regulates PCNA binding and proliferation of endothelial cells. *Mol Cell Biol* **21(16)**:5644-5657
470   DOI:10.1128/MCB.21.16.5644-5657.2001.

471   Saito R, Smoot ME, Ono K, Ruscheinski J, Wang PL, Lotia S, Pico AR, Bader GD, and Ideker T. 2012. A
472   travel guide to Cytoscape plugins. *Nat Methods* **9(11)**:1069-1076 DOI:10.1038/nmeth.2212.

473   Shang D, Wu Y, Ding Y, Lu Z, Shen Y, Zhu F, Liu H, Zhu C, and Tu Z. 2018. Identification of a pyridine
474   derivative inducing senescence in ovarian cancer cell lines via P21 activation. *Clin Exp Pharmacol Physiol*
475   **45(5)**:452-460 DOI:10.1111/1440-1681.12891.

476   Siegel RL, Miller KD, and Jemal A. 2018. Cancer statistics, 2018. *CA Cancer J Clin* **68(1)**:7-30
477   DOI:10.3322/caac.21442.

478   Sieh W, Kobel M, Longacre TA, Bowtell DD, deFazio A, Goodman MT, Hogdall E, Deen S, Wentzensen N,
479   Moysich KB, Brenton JD, Clarke BA, Menon U, Gilks CB, Kim A, Madore J, Fereday S, George J,
480   Galletta L, Lurie G, Wilkens LR, Carney ME, Thompson PJ, Matsuno RK, Kjaer SK, Jensen A, Hogdall
481   C, Kalli KR, Fridley BL, Keeney GL, Vierkant RA, Cunningham JM, Brinton LA, Yang HP, Sherman
482   ME, Garcia-Closas M, Lissowska J, Odunsi K, Morrison C, Lele S, Bshara W, Sucheston L, Jimenez-
483   Linan M, Driver K, Alsop J, Mack M, McGuire V, Rothstein JH, Rosen BP, Bernardini MQ, Mackay H,
484   Oza A, Wozniak EL, Benjamin E, Gentry-Maharaj A, Gayther SA, Tinker AV, Prentice LM, Chow C,
485   Anglesio MS, Johnatty SE, Chenevix-Trench G, Whittemore AS, Pharoah PD, Goode EL, Huntsman DG,
486   and Ramus SJ. 2013. Hormone-receptor expression and ovarian cancer survival: an Ovarian Tumor Tissue
487   Analysis consortium study. *Lancet Oncol* **14(9)**:853-862 DOI:10.1016/S1470-2045(13)70253-5.

488   Taghavi N, Biramijamal F, Sotoudeh M, Moaven O, Khademi H, Abbaszadegan MR, and Malekzadeh R.
489   2010. Association of p53/p21 expression with cigarette smoking and prognosis in esophageal squamous cell
490   carcinoma patients. *World J Gastroenterol* **16(39)**:4958-4967

491   Tangjitgamol S, Manusirivithaya S, Khunnarong J, Jesadapatarakul S, and Tanwanich S. 2009. Expressions
492   of estrogen and progesterone receptors in epithelial ovarian cancer: a clinicopathologic study. *Int J Gynecol*
493   *Cancer* **19(4)**:620-627 DOI:10.1111/IGC.0b013e3181a44b62.

494   Tomczak K, Czerwinska P, and Wiznerowicz M. 2015. The Cancer Genome Atlas (TCGA): an immeasurable
495   source of knowledge. *Contemp Oncol (Pozn)* **19(1A)**:A68-77 DOI:10.5114/wo.2014.47136.

496   Torre LA, Trabert B, DeSantis CE, Miller KD, Samimi G, Runowicz CD, Gaudet MM, Jemal A, and Siegel
497   RL. 2018. Ovarian cancer statistics, 2018. *CA Cancer J Clin* DOI:10.3322/caac.21456.

498   Urban RR, Pappas TC, Bullock RG, Munroe DG, Bonato V, Agnew K, and Goff BA. 2018. Combined
499   symptom index and second-generation multivariate biomarker test for prediction of ovarian cancer in patients
500   with an adnexal mass. *Gynecol Oncol* **150(2)**:318-323 DOI:10.1016/j.ygyno.2018.06.004.

501   Urzua U, Best L, and Munroe DJ. 2010. Microarray proteomic analysis discriminates tumorigenic mouse ovarian
502   surface epithelial cells of divergent aggressive potential. *Mol Biosyst* **6(12)**:2521-2528 DOI:10.1039/c005220e.

503   van Kooten C, and Banchereau J. 2000. CD40-CD40 ligand. *J Leukoc Biol* **67(1)**:2-17

504   van Kruchten M, van der Marel P, de Munck L, Hollema H, Arts H, Timmer-Bosscha H, de Vries E, Hospers
505   G, and Reyners A. 2015. Hormone receptors as a marker of poor survival in epithelial ovarian cancer. *Gynecol*

506   *Oncol* **138(3)**:634-639 DOI:10.1016/j.ygyno.2015.06.032.

507   **Wong KK, Lu KH, Malpica A, Bodurka DC, Shvartsman HS, Schmandt RE, Thornton AD, Deavers MT,**

508   **Silva EG, and Gershenson DM. 2007.** Significantly greater expression of ER, PR, and ECAD in advanced-

509   stage low-grade ovarian serous carcinoma as revealed by immunohistochemical analysis. *Int J Gynecol Pathol*

510   **26(4)**:404-409 DOI:10.1097/pgp.0b013e31803025cd.

511   **Xiong Y, Hannon GJ, Zhang H, Casso D, Kobayashi R, and Beach D. 1993.** p21 is a universal inhibitor of cyclin

512   kinases. *Nature* **366(6456)**:701-704 DOI:10.1038/366701a0.

513   **Zhou Y, He J, Gou LT, Mu B, Liao WC, Ma C, Tang P, Zhou SJ, Zhou YJ, and Yang JL. 2012.** Expression of

514   CD40 and growth-inhibitory activity of CD40 agonist in ovarian carcinoma cells. *Cancer Immunol Immunother*

515   **61(10)**:1735-1743 DOI:10.1007/s00262-011-1194-0.

516

517

Figure 1

Characterization of MOSE-I and MOSE-II cells *in vitro*.

A, Bright-field inverted microscopy. Cells were grown at Passage 20 for MOSE-I and Passage 90 for MOSE-II and then photographed at a magnification of 100×. B, The soft agar colony formation assay. MOSE-I (passage 20) and MOSE-II (passage 90) were grown in the soft agar for 7 days and photographed (magnification, 100×). C, The plate colony formation assay. MOSE-I (passage 20) and MOSE-II (passage 90) were grown for 14 days and stained with crystal violet solution and photographed (magnification, 100×). The graphs were quantified data of the colony formation assay. **$p <0.01$ and ***$p <0.0001$ analyzed by Student's *t* test. The data on E and D were generated by the Image J software, while the data on F were from the EVOS XL imaging system.
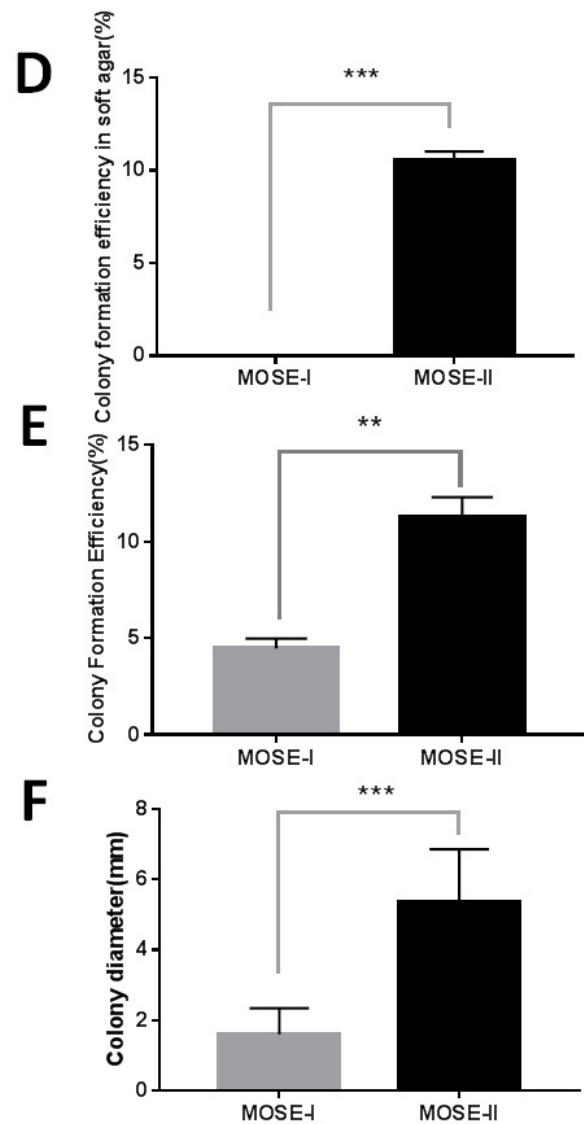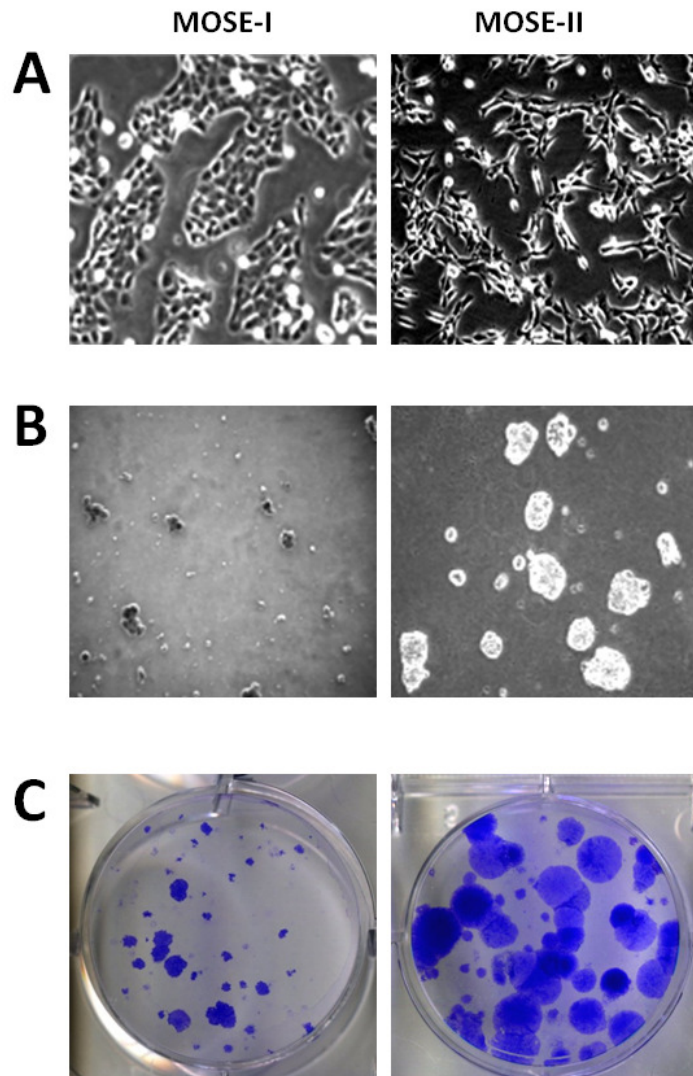
Figure 2

Identification of DEGs using Volcano plots.

The X-axis indicates the fold change (logs value), whereas the Y-axis shows the *p* values (logs value). Each symbol represents a different gene, and the red/green color shows the up- or downregulated genes falling under different criteria (*p* value and fold change threshold). A *p* value <0.05 is considered as statistically significant, whereas the four fold changes were set as the threshold.
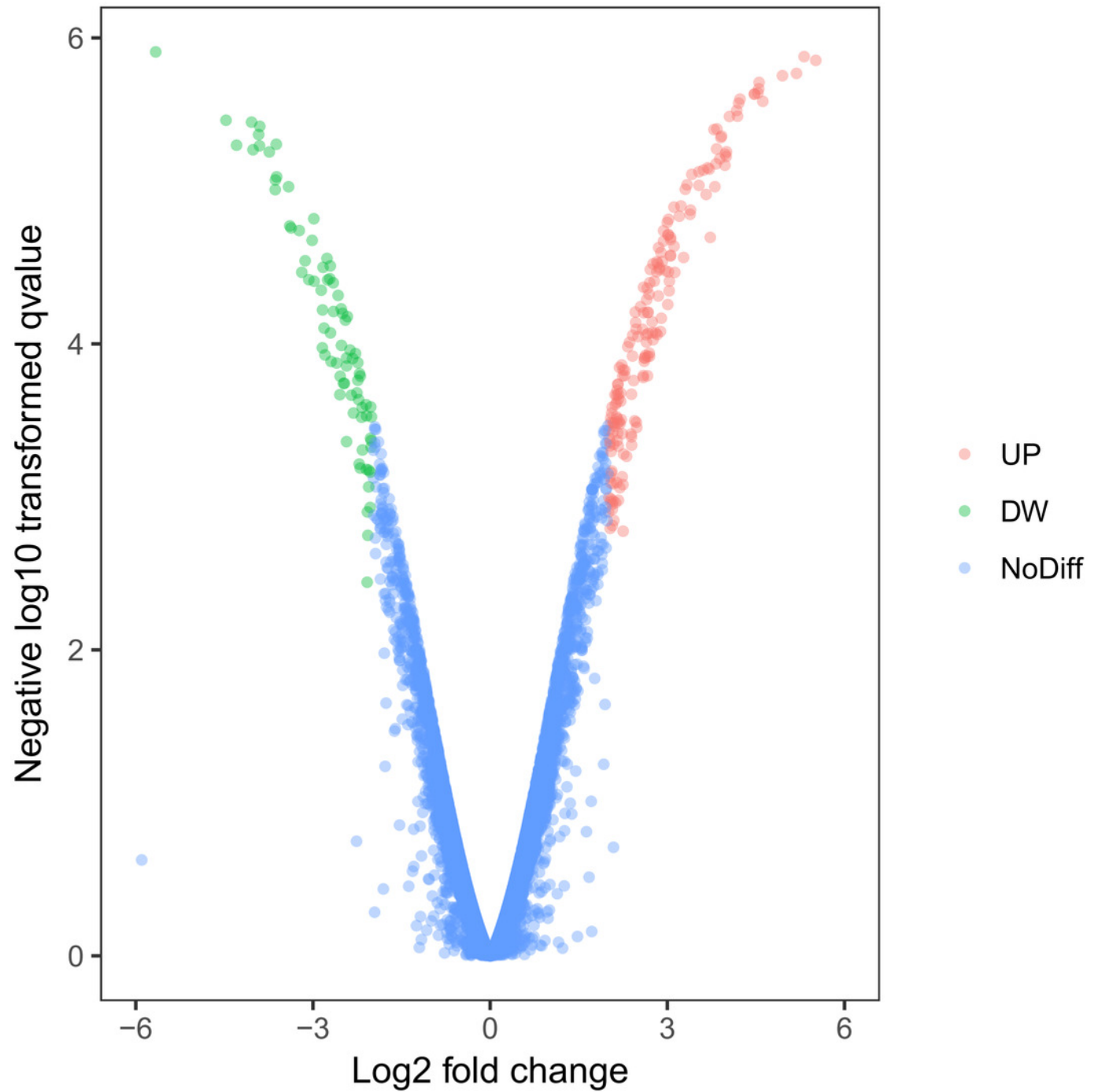
DEGs between MOSE-I and MOSE-II cells.

Gene name	Log2 fold	P values
Up-regulated genes		
Ccbe1	5.514199	1.4E-06
Sfrp2	5.316823	1.32E-06
Cntnap2	5.187267	1.7E-06
Cd55	4.949248	1.76E-06
9930013L23Rik	4.617182	2.6E-06
Ephx1	4.554543	1.95E-06
Gnai1	4.548394	2.15E-06
Ctla2a	4.534042	2.29E-06
Csgalnact1	4.478922	2.32E-06
Ahsp	4.473507	2.34E-06
Pkhd1l1	4.230823	2.51E-06
Thy1	4.208894	2.67E-06
Apoe	4.188801	3.25E-06
Tmem45a	4.175247	2.98E-06
Scg5	4.052742	3.26E-06
Slc47a1	4.001494	5.55E-06
Akr1c13	3.99621	5.96E-06
Nxnl2	3.980449	5.75E-06
Zfp385b	3.975438	6.79E-06
D630010B17Rik	3.920202	4.38E-06
Down-regulated genes		
Cst12	-5.66249	1.23E-06
Pcolce2	-4.47177	3.45E-06
Serpina3g	-4.29413	5.03E-06
Aif1l	-4.03994	3.55E-06
Tmem79	-4.01531	5.38E-06
Emb	-3.91989	4.28E-06
1810065E05Rik	-3.90506	5.07E-06
Kcnk1	-3.90055	3.78E-06
D0H4S114	-3.73926	5.56E-06
Pip5k1b	-3.01345	2.1E-05
Ano1	-3.07047	3.8E-05
Coro2b	-3.13207	2.86E-05
Cbfa2t3	-3.18901	3.41E-05
Glipr1	-3.23211	1.82E-05
Ms4a3	-3.63888	9.81E-06
Slain1	-3.63583	8.48E-06
Gmps	-3.62074	4.96E-06
Foxc2	-3.61526	8.09E-06
Emp1	-3.41282	9.39E-06
Nkx2-3	-3.39217	1.69E-05

The hub genes with the node degree >5.

number	Gene name	Node Degree	Regulation
1	Egfr	26	up
2	Acta2	23	down
3	Stat3	20	up
4	Cd40	12	up
5	Cd34	11	up
6	PR	11	up
7	Isg15	11	up
8	Serpinb1a	10	up
9	Rhobtb1	10	up
10	Gmps	9	down
11	Gnai1	9	up
12	Cd24a	8	down
13	Ptk2b	8	up
14	Irf7	8	up
15	Igf2	8	up
16	P21	8	up
17	Usp18	8	up
18	Apoe	7	up
19	Gnaz	7	up
20	Col3a1	7	up
21	Pdgfb	7	down
22	Socs2	7	up
23	Thbs1	6	up
24	Rhbdl3	6	down
25	Thy1	6	up
26	Irgm2	6	up
27	Gbp2	6	up
28	Figf	6	up
29	Fgf10	6	down
30	Rasl11a	5	up
31	Rasd2	5	up
32	Il4ra	5	up
33	Serpinb9b	5	down
34	Ccnd1	5	down
35	Fgfr2	5	up

Figure 3

Functional and pathway enrichment analyses of DEGs-formed hub genes.

A, The Kyoto Encyclopedia of Genes and Genomes (KEGG) pathways enriched gene pathways of the DEGs-formed hub genes. B, The Gene Ontology (GO) terms of DEGS related to the biological process. C, The GO terms of DEGS related to the cellular component. D, The GO terms of DEGS related to the molecular functions.

Figure 4
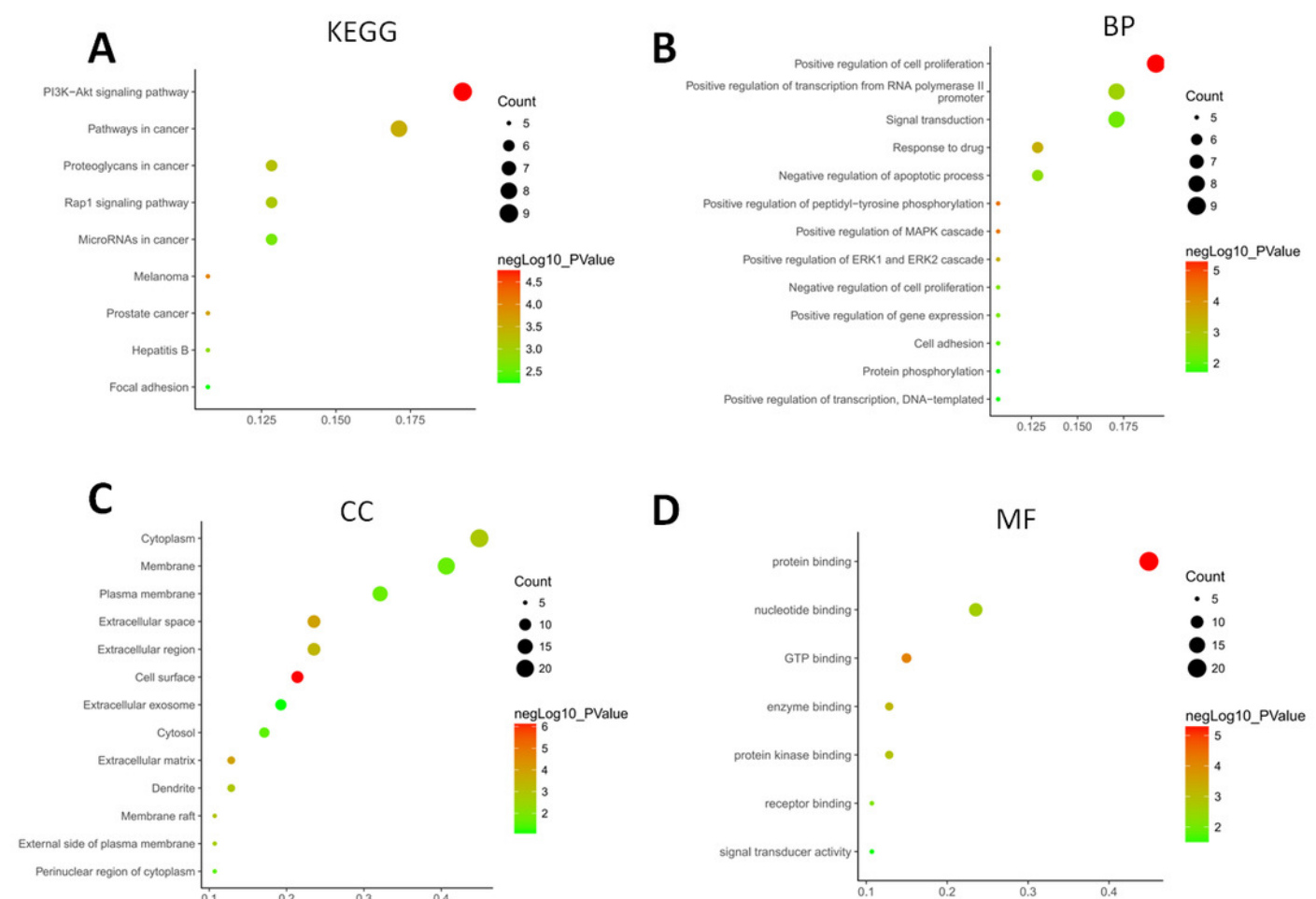
The DEGs-formed protein-protein interaction network.

The red and green circles represent up- and down-regulated genes, respectively. The node represents genes and edges for their role in connection between proteins. The nodes are colored based on in-between significance, and the higher the value, the darker the color, whereas the node size is proportional to the degree value, i.e., the higher the value, the bigger the size. The thicker line, the tighter the connection between the two proteins.
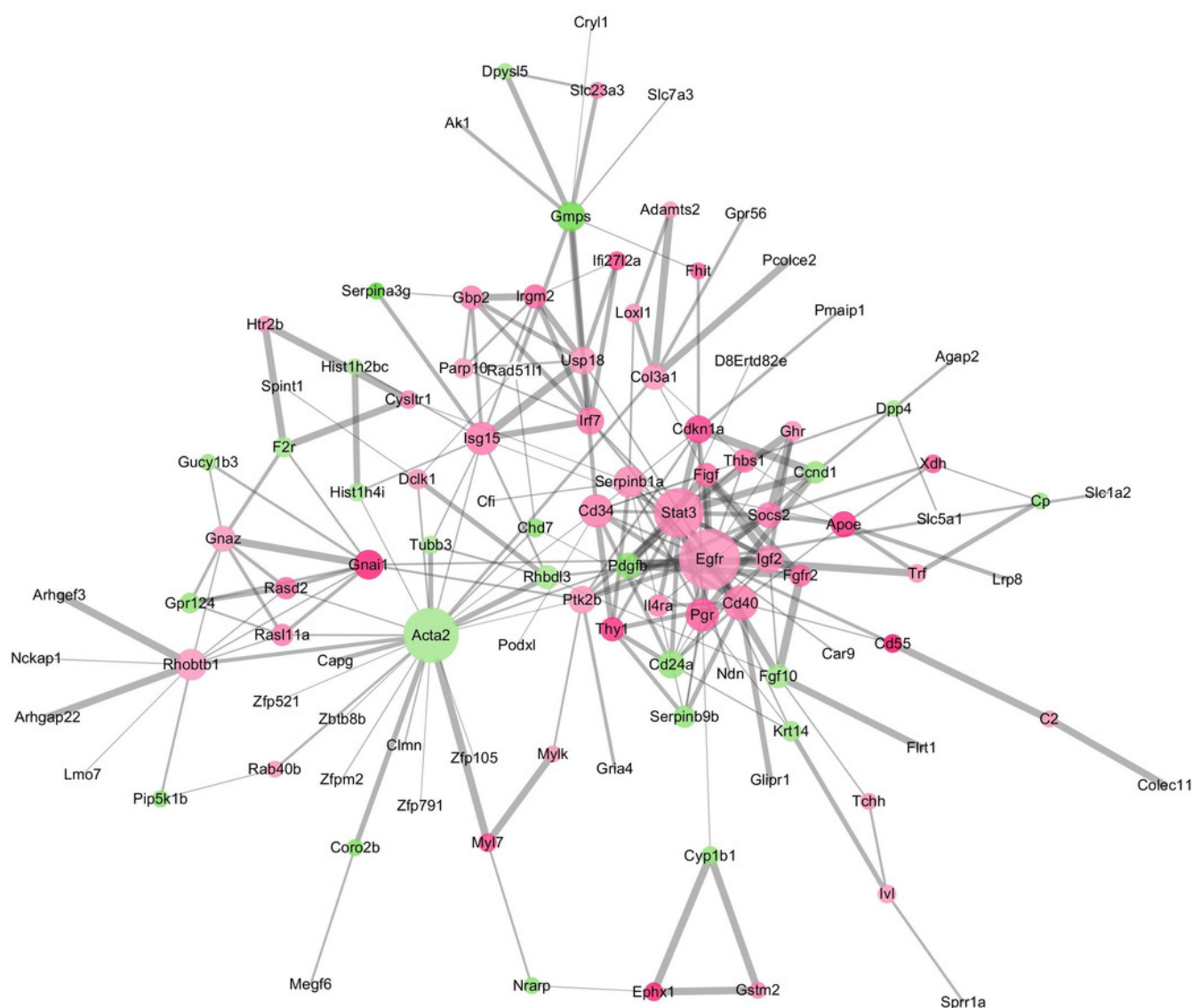
Figure 5

Identification and association of the top four-hub genes with survival of ovarian cancer patients.

A, The Oncoprint analysis to identify the four top hub genes. The cBioPortal represented the proportion and distribution of samples with alterations in hub genes. The graph is cropped to exclude samples without gene alterations or genetic alterations on the right. The red color indicates gene amplification, while the blue color represents gene deletion and the pink color gene up-regulation. B, The Kaplan-Meier curves of overall survival (OS) stratified by altered expression of these four genes. C, The Kaplan-Meier curves of disease-free survival (DFS) stratified by altered expression of these four genes.
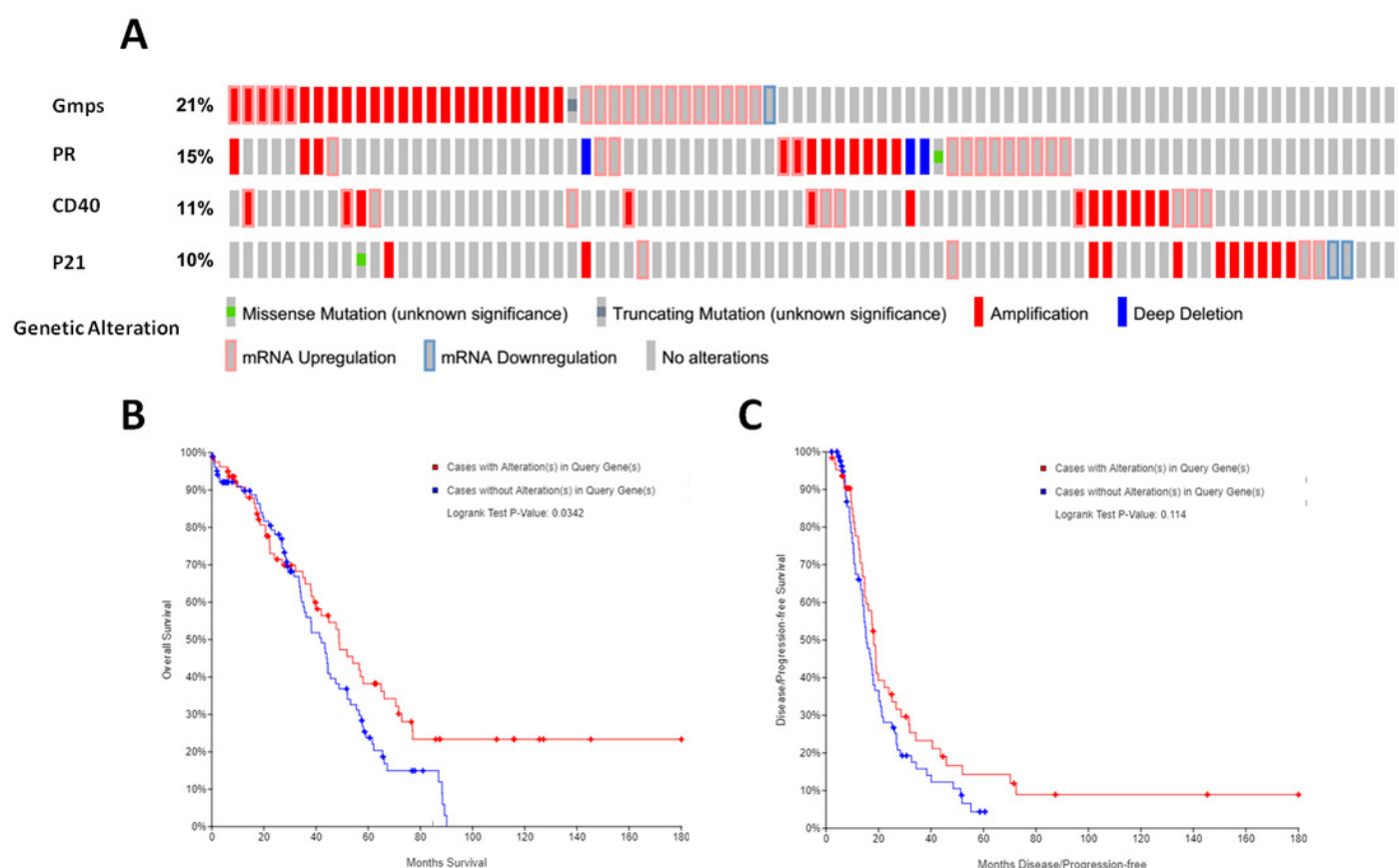
Figure 6

Differential GMPS, PR, CD40, and p21 expression between ovarian cancer and normal tissues and association with recurrence-free survival of ovarian cancer patients.

A-D, The Kaplan-Meier curves of recurrence-free survival (RFS) stratified by altered expression of these four genes. E-H, Differential expression of GMPS, PR, CD40, and p21 between ovarian cancer and normal tissues.